ON THE WIND-DRIVEN OCEAN CIRCULATION

By Walter H. Munk

Institute of Geophysics and Scripps Institution of Oceanography, University of California[1]

(Manuscript received 24 September 1949)

ABSTRACT

Streamlines of oceanic mass transport are derived from solutions to a vertically integrated vorticity equation which relates planetary vorticity, lateral stress curl, and the curl of the stress exerted by the winds on the sea surface. These solutions account for many of the gross features of the general ocean circulation, and some of its details, on the basis of the observed mean annual winds.

The solution for *zonal winds* (section 3) gives the main gyres of the ocean circulation. The northern and southern boundaries of these gyres are the west wind drift, the equatorial currents, and equatorial countercurrent. They are determined by the westerly winds, the trades, and the doldrums, respectively. For each gyre the solution gives the following observed features (from west to east): a concentrated current (*e.g.*, the Gulf Stream), a countercurrent, boundary vortices (the Sargasso Sea), and a steady compensating drift. Using mean Atlantic zonal winds, the solution yields a transport for the Gulf Stream of 36 million metric tons per second, compared to 74 million as derived from oceanographic observations. The discrepancy can probably be ascribed, at least in part, to an underestimate of the wind stress at low wind speeds (Beaufort 4 and less) as derived from the relationship now generally accepted.

The solution for *meridional winds* (section 5) accounts for the main features of the current system off California. For a *circular wind system* (section 8) the solution gives a *wind-spun* vortex which is displaced westward in relation to the wind system, in agreement with observations in the Northeast Pacific high-pressure area.

Based on these three solutions, a general nomenclature of ocean currents is introduced (section 9), applicable to all oceans regardless of hemisphere, and suggestive of the meteorologic features to which the currents are so closely related. In the light of this general system, the circulations of the northern and southern hemispheres, and of the North Atlantic and North Pacific are compared (section 10). Rossby's jet-stream theory of the Gulf Stream, and Maury's theory of thermohaline circulation are discussed, and it is concluded that the circulation in the upper layers of the oceans are the result chiefly of the stresses exerted by the winds.

1. Introduction

This study is a resumption of Ekman's (1923; 1932) intensive effort to account theoretically for the main features in the general ocean circulation. The temptation to reopen this problem is provided by three recent developments: (*a*) Rossby's (1936) introduction of lateral stresses associated with the horizontal exchange of large eddies; (*b*) Sverdrup's (1947) computation of the equatorial countercurrents in a baroclinic ocean from the known wind stress; and (*c*) Stommel's (1948) explanation of the westward intensification of a wind-induced circulation in terms of the variation of the Coriolis parameter with latitude.

In Ekman's and Stommel's model the ocean is assumed homogeneous, a case in which the currents extend to the very bottom. Not only is this in contrast with observations, according to which the bulk of the water transport in the main ocean currents takes place in the upper thousand meters, but it also leads to mathematical complications which rendered Ekman's analysis very difficult, and forced Stommel to resort to a rather arbitrary frictional force along the bottom.

To avoid these difficulties, we retain Sverdrup's integrated mass transport as the dependent variable. This device makes it possible to examine the more general case of a baroclinic ocean without having to specify the nature of the vertical distributions of density and current. In recognition of the evidence that currents essentially vanish at great depths, we shall depend on lateral friction for the dissipative forces. From Stommel we retain the rectangular boundaries, although we extend the basin to both sides of the equator and deal with the *observed* wind distribution rather than a simple sinusoidal distribution.

2. The differential equation of mass transport

Let the x-axis point eastward along the equator, the y-axis northward, and the z-axis vertically upwards from a level surface (assumed plane) just beneath the sea surface (unit vectors $\mathbf{i}$, $\mathbf{j}$, $\mathbf{k}$). For the present, the nonlinear inertial terms are considered negligible, an assumption which will be examined in section 10. The equations of steady horizontal motion for a unit

[1] Contribution from the Scripps Institution of Oceanography, New Series, No. 462. This paper was prepared partly under a Guggenheim Fellowship at the University of Oslo, partly with the support of the Office of Naval Research.

volume are

$$\nabla_H p + f\mathbf{k} \times (\rho \mathbf{v}_H) - \frac{\partial}{\partial x}\left(A'_H \frac{\partial \mathbf{v}_H}{\partial x}\right) - \frac{\partial}{\partial y}\left(A'_H \frac{\partial \mathbf{v}_H}{\partial y}\right) - \frac{\partial}{\partial z}\left(A'_V \frac{\partial \mathbf{v}_H}{\partial z}\right) = 0, \quad (1)$$

where $\nabla_H = \mathbf{i}\,\partial/\partial x + \mathbf{j}\,\partial/\partial y$, p is pressure, ρ is density, $\mathbf{v}_H = \mathbf{i}\,v_x + \mathbf{j}\,v_y$ is the two-dimensional (horizontal) velocity vector, and $f = 2\omega \sin \varphi$ is twice the vertical component at latitude φ of the earth's angular velocity ω. Observations have shown that A'_V, the dynamic eddy viscosity associated with vertical shear, is different from A'_H, the eddy viscosity pertaining to horizontal shear, the two coefficients bearing a ratio rather larger than that of the width of the ocean currents to their depth. We shall assume A'_H horizontally isotropic, neglecting variations that might be related to differences between zonal and meridional motions of of large horizontal eddies on a rotating earth.

The equations of motion will be integrated from some constant depth, $-h$, beneath which the motion and horizontal pressure gradients essentially vanish (Sverdrup, 1947), to the surface, $z = z_0(x, y)$. Let

$$P = \int_{-h}^{z_0} p\, dz, \qquad \mathbf{M}_H = \int_{-h}^{z_0} \rho\, \mathbf{v}_H\, dz, \quad (2a, b)$$

designate the integrated pressure and mass transport. Then

$$\int_{-h}^{z_0} \nabla_H p\, dz = \nabla_H P - p_{z_0} \nabla_H z_0,$$

where p_{z_0} is the atmospheric pressure and $\nabla_H z_0$ is the gradient of the sea surface. The second term is negligible for the present investigation.

The integration of the horizontal shearing forces is more cumbersome. The simplest form is $A_H \nabla^2_H \mathbf{M}$, where A_H is an effective kinematic eddy viscosity which is assumed independent of x and y. There is no evidence to indicate that the complicated expression given by a complete integral with a variable $A_H = A'_H/\rho$ would be a more accurate description of the forces. Finally

$$\int_{-h}^{z_0} \frac{\partial}{\partial z}\left(A'_V \frac{\partial \mathbf{v}_H}{\partial z}\right) dz = \left[A'_V \frac{\partial \mathbf{v}_H}{\partial z}\right]_{z_0} - \left[A'_V \frac{\partial \mathbf{v}_H}{\partial z}\right]_{-h} = \boldsymbol{\tau}, \quad (3)$$

where $\boldsymbol{\tau}$ is the stress applied by the wind on the sea surface. In most ocean areas it is adequate to select a depth h of 1000–2000 meters, which is comfortably above the sea bottom. The foregoing equation could be used even where the current extends to the bottom, provided $\boldsymbol{\tau}$ would then designate surface stress minus bottom stress.

With the understanding that all operators and vectors have only horizontal components, the subscript H can be dropped, and the integrated equations of motion become

$$\nabla P + f\mathbf{k} \times \mathbf{M} - \boldsymbol{\tau} - A\,\nabla^2 \mathbf{M} = 0. \quad (4)$$

The vertical integration enables us, therefore, to avoid any assumptions regarding the variation of A'_V with depth, and to postpone an examination of the density and velocity structure in depth.

The surface kinematic boundary condition requires w_{z_0} to vanish for steady state; furthermore it has been assumed that $w_{-h} = 0$. Therefore $\nabla \cdot \mathbf{M} = 0$, or $M_x = -\partial\psi/\partial y$, $M_y = \partial\psi/\partial x$, *i.e.*,

$$\mathbf{M} = \mathbf{k} \times \nabla\psi, \quad (5)$$

where ψ is the mass-transport stream function (dimensions: mass/time). Substituting ψ into (4) and performing the curl operation to eliminate P gives the differential equation of mass transport

$$\boxed{(A\nabla^4 - \beta\,\partial/\partial x)\psi = -\operatorname{curl}_z \boldsymbol{\tau},} \quad (6)$$

where $\operatorname{curl}_z \boldsymbol{\tau}$ is the vertical component of the wind-stress curl, $\nabla^4 = \partial^4/\partial x^4 + 2\,\partial^4/\partial x^2 \partial y^2 + \partial^4/\partial y^4$ is the biharmonic operator, and $\beta = df/dy$ is the rate of change northward of twice the vertical component of the earth's angular velocity.

Equation (6) is an integrated version of the vorticity equation. Ekman calls $\beta\,\partial\psi/\partial x = \beta M_y$ the planetary vorticity. Accordingly, the vorticity equation (6) expresses a balance between lateral stress curl, planetary vorticity and wind-stress curl.

For boundary conditions we choose

$$\psi_{\text{bdry}} = 0, \qquad (\partial\psi/\partial\nu)_{\text{bdry}} = 0, \quad (7a, b)$$

where ν is normal to the boundary. The first equation states that the boundary itself is a streamline (whose value is arbitrarily selected as zero); the second equation states that no slippage takes place against the boundary.

The problem is to solve (6) subject to boundary conditions (7). Hidaka (1949) has given the formal solution employing the transformation into a variational problem. There is a remarkable analogy between this problem and a problem arising in the theory of elasticity (Rayleigh, 1893; Love, 1944, p. 464). The deflection ψ of a plate of uniform flexural rigidity A, clamped at its boundaries and subjected to a load $-\operatorname{curl}_z \boldsymbol{\tau}$ is governed by

$$A\nabla^4\psi = -\operatorname{curl}_z \boldsymbol{\tau}, \quad (8)$$

subject to boundary conditions (7). Equation (6) reduces to this form when the planetary vorticity is negligible, a condition that might arise in high latitudes ($\beta \approx 0$) and for quasizonal flow ($M_y \approx 0$). The analogy suggests experimental methods for finding streamlines under complex wind stress and boundary conditions.

3. Solution for zonal winds

A rectangular ocean is assumed, extending from $x = 0$ to $x = r$, and from $y = -s$ to $y = +s$. One may think that such an arbitrary choice of ocean boundaries would make it impossible to deal with actual conditions. Yet the proper solution for the *main features* in the ocean circulation can be expected to be rather insensitive to the choice of boundaries, because these main features are similar in all oceans (table 3) although the boundaries are not. The boundary conditions (7) become

$$\psi = 0, \qquad \partial\psi/\partial x = 0, \qquad \text{for } x = 0, \quad x = r; \tag{9}$$

$$\psi = 0, \qquad \partial\psi/\partial y = 0, \qquad \text{for } y = -s, y = s. \tag{10}$$

For a *zonal* wind circulation ($\tau_y = 0$) the stress on the sea surface in the interval $-s < y < +s$ can be written as a sum of terms like

$$\tau_{xn} = a \cos ny + b \sin ny + c$$

where $n = j\pi/s$, $j = 1, 2, \cdots$ *etc.* The vertical component of the wind-stress curl is then a sum of terms like

$$\text{curl}_{zn}\, \tau = -\partial\tau_{xn}/\partial y = n(a \sin ny - b \cos ny), \tag{11}$$

and the particular integral of (6) becomes

$$\psi_{pn} = -n^{-3}A^{-1}(a \sin ny - b \cos ny) = -n^{-4}A^{-1}\,\text{curl}_{zn}\,\tau. \tag{12}$$

Let $k = \sqrt[3]{\beta/A}$ designate the *Coriolis-friction* wave number, assumed constant. The solution to the homogeneous equation

$$(\nabla^4 - k^3\,\partial/\partial x)\psi_{hn} = 0, \tag{13}$$

can be written as a product of $(a \sin ny - b \cos ny)$ and a function of x. For later convenience we choose the form

$$\psi_{hn} = \psi_{pn}(rAn^4\beta^{-1}X_n - 1), \tag{14}$$

where X is a function of x to be determined below. The complete integral equals

$$\psi_n = \psi_{pn} + \psi_{hn} = rAn^4X_n\beta^{-1}\psi_{pn},$$

or

$$\psi_n = -rX_n\beta^{-1}\,\text{curl}_{zn}\,\tau. \tag{15}$$

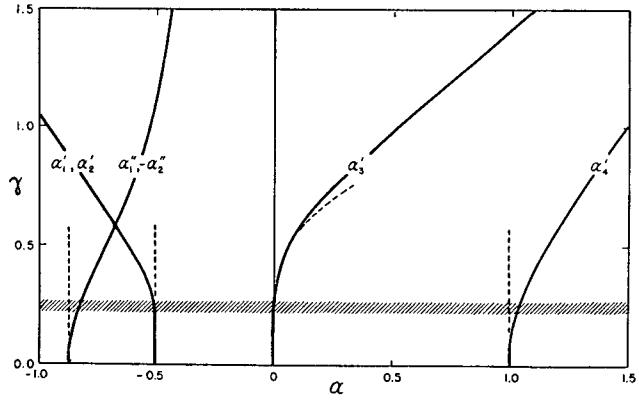

FIG. 1. Roots $\alpha' + i\alpha''$ to characteristic equation (16). The dashed lines give the asymptotic solutions for $\gamma \ll 1$ which have been applied to the large scale features ($\gamma < 0.25$) in the ocean circulation.

It follows from (12), (13) and (14) that the function $X_n(x)$ must obey the differential equation

$$X'''' - 2n^2X'' - k^3X' + n^4X = \beta/rA = k^3/r,$$

which yields

$$(\gamma_n{}^4kr)X = 1 + \tfrac{1}{2}(p_1 + ip_2)e^{\alpha_1 kx} + \tfrac{1}{2}(p_1 - ip_2)e^{\alpha_2 kx} + p_3e^{\alpha_3 kx} + p_4e^{\alpha_4 kx},$$

where $\gamma = n/k$ is the essential nondimensional number in this investigation, and where α_1, α_2, α_3, α_4 are the roots of the characteristic equation

$$(\alpha^2 - \gamma_n{}^2)^2 = \alpha. \tag{16}$$

This equation has two complex roots, $\alpha_1' + i\alpha_1''$, $\alpha_2' + i\alpha_2''$, and two real roots, α_3', α_4' (fig. 1). For small values of γ,

$$\begin{aligned} \alpha_1 &= -\tfrac{1}{2}(1 + i\sqrt{3}), & \alpha_3 &= \gamma_n{}^4, \\ \alpha_2 &= -\tfrac{1}{2}(1 - i\sqrt{3}), & \alpha_4 &= 1, \end{aligned} \tag{17}$$

as shown by the dotted lines in fig. 1. The boundary conditions (9) give

$$-p_1 \approx -p_2\sqrt{3} \approx 1 + p_3 \approx p_4 \approx \gamma_n{}^4kr, \tag{18}$$

provided

$$\gamma_n{}^4 \ll 1, \qquad e^{-kr} \ll 1, \qquad e^{-\gamma_n{}^4kr} \approx 1 - \gamma_n{}^4kr. \tag{19}$$

Subject to these approximations,

$$X = \underbrace{-Ke^{-\frac{1}{2}kx}\cos\left(\frac{\sqrt{3}}{2}kx + \frac{\sqrt{3}}{2kr} - \frac{\pi}{6}\right)}_{\text{west}} + \underbrace{1 - \frac{1}{kr}[kx - e^{-k(r-x)} - 1]}_{\text{east}} \tag{20}$$

$$\frac{X'}{k} = \underbrace{Ke^{-\frac{1}{2}kx}\sin\left(\frac{\sqrt{3}}{2}kx + \frac{\sqrt{3}}{2kr}\right)}_{\text{west}} \underbrace{- \frac{1}{kr}[1 - e^{-k(r-x)}]}_{\text{central}}, \tag{21}$$

where $K = 2/\sqrt{3} - \sqrt{3}/kr$. The meaning of the horizontal braces will be discussed later.

The important thing to notice is that, to the present degree of approximation, X does not depend on n; *i.e.*, that the response of the current to the zonal wind stress is without distortion in the y-direction for

$\gamma \ll 1$. Equation (15) can therefore be written

$$\boxed{\psi = -rX\beta^{-1}\,\mathrm{curl}_z\,\tau,} \qquad (22)$$

and the stream function computed directly from the observed (zonal) stress without expanding the stress in a Fourier series, provided such a series converges so rapidly that for all significant terms conditions (19) are fulfilled. Whether this is the case can usually be told by inspection. Anticipating the numerical values $k = .016$ km^{-1}, $r = 6000$ km, conditions (19) for 10 per cent accuracy in ψ give $\gamma < 0.25$, corresponding to a minimum zonal wave length $2\pi/n$ of about 1500 km. For the mean annual stress distribution (fig. 2) the shortest wave length of the important N-S variations is the distance between the northern and southern trades, 4000 km. *The approximations leading up to (22) appear to be valid for a study of the general ocean circulation as it is related to the general atmospheric circulation.*

For stationary compact cyclones and sharp fronts with *overtones* of less than 1500 km wave length ($\gamma > 0.25$), it is necessary to compute separately the components ψ_n for each component wind stress τ_n according to equation (15), and to sum. The roots α can be read off fig. 1 and the p's determined by the original boundary conditions (9).

There remain the conditions (10) at the northern and southern boundaries. We note (fig. 9) that the winds are weak at 60°–70° latitudes, and we shall satisfy (10) by assuming $\mathrm{curl}_z\,\tau$ and its derivative to approach zero at these boundaries. It must be admitted that this easy way of satisfying boundary conditions is aided by the present lack of adequate wind data in high latitudes.

To the extent to which these conditions on $\mathrm{curl}_z\,\tau$ are not satisfied there must be deviations from the present solution, but we may expect these deviations to be restricted to relatively narrow zones adjacent to the northern and southern boundaries for the following reasons: The general circulations in the Atlantic and Pacific Oceans are in a very rough sense symmetrical with respect to the equator (except for an asymmetry related to the asymmetry of the wind circulation), whereas the boundaries are not. To the south all oceans open into the Antarctic Sea, to the north they are practically closed. Even the Indian Ocean, with its northern boundary only 1000–2000 km north of the equator, has about the same circulation in its central and southern parts as the Atlantic and Pacific.

It is none the less possible that important features have escaped us by the present incomplete treatment,

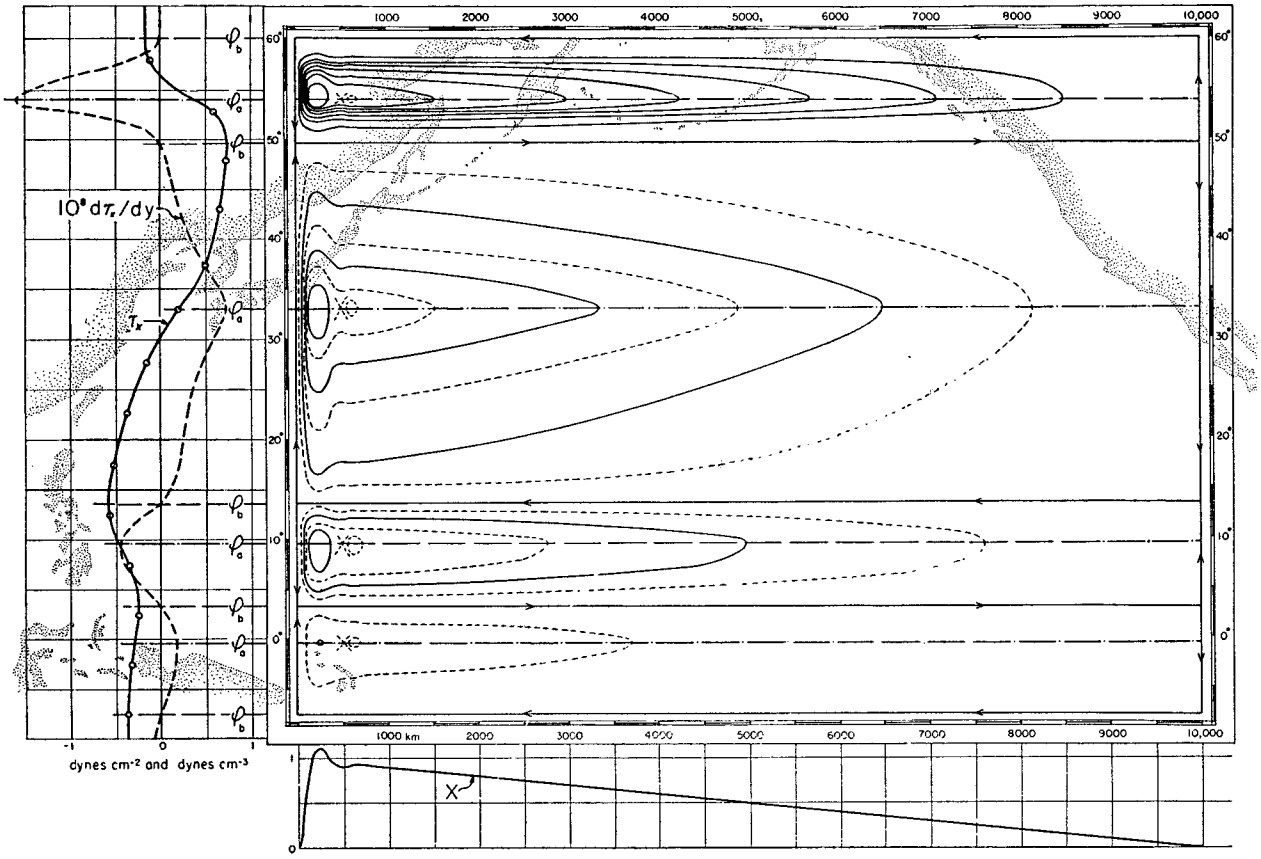

FIG. 2. The mean annual zonal wind stress $\tau_x(y)$ over the Pacific and its curl $d\tau_x/dy$ are plotted on the left, the function $X(x)$ on the lower part. These functions have been combined graphically according to equation (22) to give mass transport streamlines $\psi(x, y)$. The transport between adjacent solid lines is 10×10^{12} g sec^{-1}, or 10 million metric tons sec^{-1}. The total transport between the coast and any point x, y is $\psi(x, y)$. The chart of the Pacific has a uniform distance scale throughout. In the relatively narrow northern portion, the transport is greatly exaggerated.

and we hope to be able to give a complete numerical solution (for actual boundaries) at a later time. The similar but much simpler problem of a rectangular plate clamped at its edges and subject to a uniform load (equations 8, 9, 10 with $\text{curl}_z \tau$ constant) has received considerable attention, yet no complete theoretical solution has been found, and recourse has had to be made to rather elaborate numerical methods (Love, 1944, pp. 493–497). We note, however, that the solution in the vicinity of the transverse axis (corresponding to low and middle latitudes) for a plate which is more than twice as long as broad is practically the same as if the length were infinite.

4. Zonal wind currents

The wind stress has been computed for the North Pacific and the North and Central Atlantic for each month and 5-degree quadrangle. The source material consisted of the wind roses on the U. S. Hydrographic Office Pilot Charts of the North Pacific Ocean, the summary of Marine Data Cards of the U. S. Weather Bureau, and the Monthly Meteorological Charts of the Atlantic Ocean prepared by the Meteorological Office, Air Ministry, London. The variability of the wind and the hydrodynamic character of the sea surface has been taken into account in the manner described by Reid (1948). Fig. 2 shows the mass transport streamlines $\psi(x, y)$ in a rectangular ocean computed from (22) for the mean annual *zonal* winds over the Pacific. The topography of the free surface and of other isobaric surfaces is related to the ψ-topography, the relationship depending however on the vertical density structure. For the equatorial Pacific, Reid (1948b) has successfully used a simple model of vertical density distribution consisting of a homogeneous layer of density ρ_0 and thickness h' above an *exponential* layer of density $\rho_{-\infty} - (\rho_{-\infty} - \rho_0) \exp(1 + z/h')$. He finds

$$P + \textit{constant} = \tfrac{5}{8} g \frac{\rho_0^2}{\rho_{-\infty} - \rho_0} z_0^2 = (5/2) g (\rho_{-\infty} - \rho_0) h'^2 \approx f\psi \quad (23)$$

for the elevation z_0 of the surface above, and the depression of h' beneath their mean level.

The major ocean gyres.—The zonal wind system divides the ocean circulation into a number of gyres, each bounded by latitudes φ_b for which $M_y = 0$, or by (22),

$$\text{curl}_z \tau = 0 \text{ at } \varphi = \varphi_b.$$

The major dividing lines between gyres correspond to the latitudes of maximum west winds, of the northerly and southerly trades, and of the doldrums (fig. 2). These compare favorably with those determined from oceanographic observations.

The latitudinal *axis* of each gyre may be defined by $M_x = 0$, or

$$\frac{d}{dy} \frac{\text{curl}_z \tau}{\beta} = 0 \approx \frac{d^2 \tau_x}{dy^2} \quad \text{at} \quad \varphi = \varphi_a.$$

The Atlantic Sargasso Sea is associated with the inflection point in the mean wind stress curve between the westerly winds and the northeasterly trades.[2] The inflection points between the doldrums and the northern and southern trades determine the boundaries of the equatorial countercurrent.

The western currents.—Along any fixed latitude, ψ varies with X only, and the curves $X(x)$ and $X'(x)$ in fig. 3 can be interpreted as the north–south component of transport, and transport per unit length, drawn to an arbitrary scale. For definiteness, consider sections at latitudes φ_a through the center of gyres.

When X and X' are computed from (20) and (21), it is found that the equations fall naturally into three parts, each of which dominates in a given sector. At

[2] The dependence $r(y)$ of the width of the ocean basin on latitude somewhat modifies this conclusion when applied to non-rectangular ocean basins (Munk and Carrier, 1950).

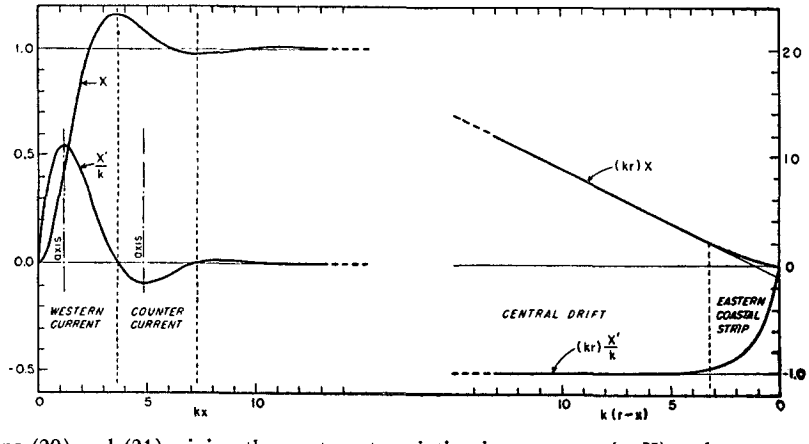

FIG. 3. Plot of equations (20) and (21), giving the west–east variation in transport ($\sim X$) and transport velocity ($\sim X'$) from the western shore ($x = 0$) to the eastern shore ($r - x = 0$). The scale for the central and eastern solutions is exaggerated relative to the scale for the western solution.

the western edge of the ocean $x \ll r$, and

$$X_W = -\frac{2}{\sqrt{3}} e^{-\frac{1}{2}kx} \cos\left(\frac{\sqrt{3}}{2}kx - \frac{\pi}{6}\right) + 1, \quad (20W)$$

$$\frac{X'_W}{k} = \frac{2}{\sqrt{3}} e^{-\frac{1}{2}kx} \sin\frac{\sqrt{3}}{2}kx, \quad (21W)$$

representing slightly *underdamped* oscillations of wave length

$$L_W = \frac{4\pi}{\sqrt{3}k} = \frac{4\pi}{\sqrt{3}\sqrt[3]{\beta}} A^{\frac{1}{3}}. \quad (24)$$

TABLE 1. Extrema of X_W and X'_W.

	Location (see fig. 3)			
	Western current axis	Western current limit	Counter-current axis	Counter-current limit
x/L_W	1/6	3/6	4/6	1
X_W	0.45	1.17	1.09	0.97
X'_W/k	0.55	0.00	−0.09	0.00

Table 1 gives the locations and values of the first few extrema. A remarkable feature is a countercurrent east[3] of the main current, whose magnitude is exp $(-\pi/\sqrt{3})$, or 17 per cent of that of the main current. There can be little doubt that such countercurrents exist, although this fact has been obscured in some instances by the smoothing of data. In comparing the Kuroshio and the Gulf Stream, Wüst (1936, p. 56) remarks that (writer's translation) ". . . both currents are accompanied by a countercurrent on their right which attains surface velocities up to approximately 20 cm sec^{-1}. This current, which is found for all Gulf Stream profiles based on *Atlantis* and *Dana* observations is a most peculiar phenomenon." According to Wüst's figures, the maximum speeds of the countercurrents average 19 per cent of that of the main currents, compared to the theoretical value of 17 per cent. In describing the Gulf Stream, Iselin (1936, p. 43) states that ". . . the western margin of the current is extremely abrupt, while on the eastern side the velocity decreases gradually." The theory places the current axis twice as near the western as the eastern side.

The function X_W (fig. 3) compares favorably with the transport function ψ (fig. 4) across the Gulf Stream and Kuroshio computed from oceanographic data according to the equations

$$\frac{f\psi}{\bar{\rho}} = Q = \int_{-h}^{z_0} \int_{-h}^{p(z)} \delta' \, dp \, dz, \quad (25)$$

where δ' is the specific volume anomaly (Sverdrup *et al.*, 1942, p. 463), although there remain significant differences between the computed and observed transport curves, and of course between the observed currents themselves.

[3] A countercurrent on the *western* edge of the Gulf Stream has been accounted for by Rossby (1936) in his wake-stream theory. Further remarks will be found in section 10.

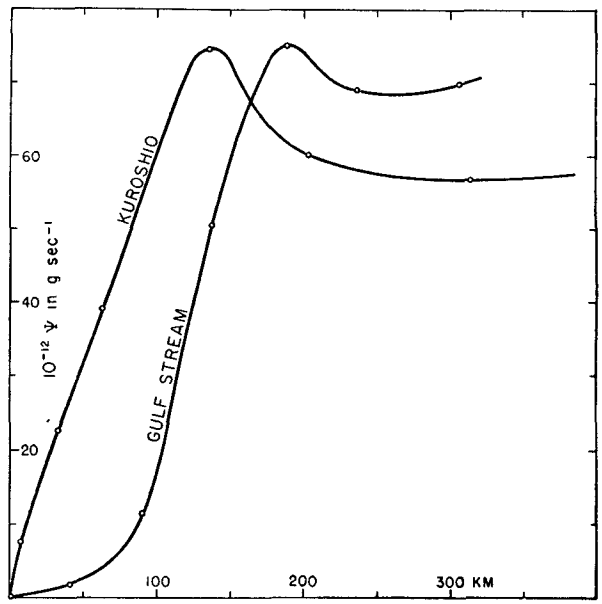

FIG. 4. The mass transport stream function ψ computed from oceanographic data across the Kuroshio and Gulf Stream. These curves should be compared to the theoretical function X on the left side of fig. 3. GULF STREAM: *Atlantis* stations 1225–1231, April 1932 (Iselin, 1936); $x = 0$ is placed at boundary between coastal water and slope water. KUROSHIO: *Mansyu* stations 429–434, January 1927 (Wüst, 1936); $x = 0$ is placed at continental shelf.

A review of oceanographic observations suggests 200 km and 250 km as typical values for the widths of the western currents and countercurrents, respectively. The corresponding values of A are 3.3×10^7 and 6.5×10^7 cm^2 sec^{-1} (equation 24), indicating perhaps an increase of A with distance from shore as might be expected on the basis of Prandtl's mixing-length theory. We shall set $A = 5 \times 10^7$ cm^2 sec^{-1}. This compares favorably with the values 4×10^7 and 7×10^7 cm^2 sec^{-1} for the region of the Atlantic equatorial countercurrent, the former determined by Montgomery (1939) from the diffusion of salt, the latter by Montgomery and Palmén (1940) from dynamic principles. One may expect, however, that the value of A varies with time and location, and that for any fixed time and location it has different values, depending on the dimensions of the phenomenon under investigation. Without any further information we shall be obliged to consider the above value as constant.

The *total* transports of the western current and countercurrent are found by substituting values for X_W from table 1 into (22):

$$\psi_{WC} = -1.17 r\beta^{-1} \operatorname{curl}_z \tau. \quad (26)$$

The resulting expressions *are independent of* A, and the transports can be computed with a relatively high degree of accuracy, being subject largely to uncertainties of the same order as those in computing wind stress. A comparison is made in table 2 between the transport values of some western currents determined from oceanographic observations, and those computed

TABLE 2. The mass transport of some western currents determined from the wind stress (equation 26) and from oceanographic observations.

Current	Lat.	$10^{13}\beta$ $cm^{-1}\,sec^{-1}$	r km	$10^{10}\frac{d\tau_x}{dy}$ g sec^{-2}	Merid. wind factor	$10^{12}\psi$ Wind stress g sec^{-1}	Oceanogr. g sec^{-1}
Gulf Stream	35°N	1.9	6,500	70	1.30	36	74[4] (55)[5]
Kuroshio Ext.	35°N	1.9	10,000	50	1.25	39	65[4]
Oyashio C.	50°N	1.5	5,500	−15	—	−6.5	−7[6]
Brazil C.	20°S	2.2	5,500	−20	—	−5.8	−5 to −10[4]

[4] Sverdrup *et al.* (1942), pp. 605–761.
[5] Adjusted for a supposed southward motion of 19×10^{12} g of slope water per second. Sverdrup *et al.* (1942), p. 679.
[6] For August (Uda, 1938).

from the zonal wind stress according to (26). The effect of the meridional wind component, which supports the zonal winds, is introduced by a meridional wind factor (see section 7)

$$-\overline{\text{curl}_z\,\tau}\;(d\bar{\tau}_x/dy)^{-1}. \qquad (27)$$

The approximation involved in permitting the "constants" β and r to assume different values at different latitudes implies that these vary slowly compared to τ and ψ. However, not even a rapid change of r introduces an appreciable error into (26); the only essential modification is a widening and corresponding weakening of the western current, determined by the inclination of the western coastline relative to the assumed north–south direction (Munk and Carrier, 1950).

The computed transport values differ from the observed values by as much as a factor of two, a discrepancy not surprising if one considers that, among other uncertainties, wind and current data are not for the same year, nor necessarily for the same time of year. On examining the possible sources of errors, one is led to ascribe some of the discrepancy to an underestimate of wind stress for low wind speeds. We shall return to this question in section 10.

The western boundary vortices (Sargasso Sea).—Beyond the countercurrent, the next term in (20) and (21) can no longer be neglected. It pivots the asymptotic solution $X = 1$ to $X = 1 - x/r$, and shifts $X'/k = 0$ to $X'/k = -1/kr$ (fig. 2, bottom). The resulting streamlines represent an exponentially decaying vortex trail centered along the axis φ_a (fig. 5). Only the two western vortices need be considered. Accordingly the Sargasso Sea (or any of the other dynamically analogous areas) is a region of relatively sluggish circulation containing a moderately strong anticyclonic vortex at the western side and a weak anticyclonic vortex near its center. The two vortices represent two humps in the sea surface which are separated by a trough with a saddle point in the vicinity of Bermuda. Reid's model (equation 23) gives 10 cm and 2 cm for the peak elevations of the western and eastern humps above the saddle point.

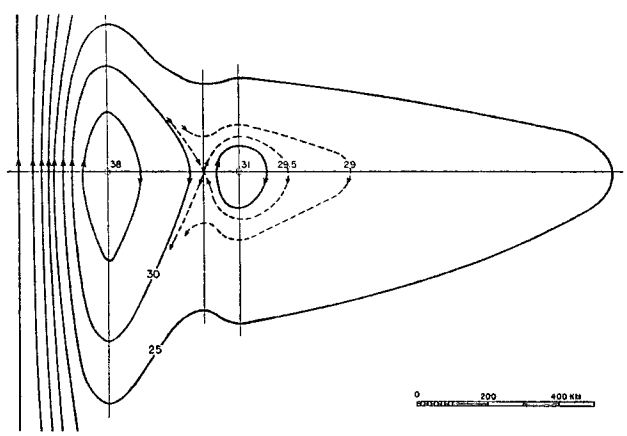

FIG. 5. The mass transport stream function in units of 10^{12} g sec^{-1} near the western boundary for mean annual zonal winds over the Atlantic. The center line is at 31°N. For comparison with the Sargasso Sea circulation, the figure should be distorted by maintaining the west–east orientation of the x-axis and rotating the y-axis clockwise until the western current and countercurrent are parallel to the coast line. (Munk and Carrier, 1950.)

Felber (1934) has analyzed the extensive observational material based on surface drifts of vessels, and his streamlines show a saddle point southwest of Bermuda. A chart of the topography of the sea surface prepared by Defant (1941) on the basis of the *Meteor* observations and preceding observations, does indeed show two humps. Recent detailed observations from closely spaced lowerings of bathythermographs, though inconclusive, are not inconsistent with the above picture.

Central ocean drift.—Away from both boundaries, the equations

$$X_C = 1 - x/r, \qquad X'_C/k = -1/kr, \qquad (20C, 21C)$$
$$M_y = \partial\psi/\partial x = \beta^{-1}\,\text{curl}_z\,\tau \qquad (28)$$

give a broad *constant* drift that compensates for the swift, shallow western currents. Equation (28) was derived by Sverdrup (1947). By dropping the lateral stress term this equation could have been written directly from (6) *without the restriction to zonal winds.* The validity of the theory in mid-ocean has been adequately confirmed by the successful application of (28) to the equatorial currents of the eastern Pacific (Sverdrup, 1947; Reid, 1948a, b).

Eastern coastal strip.—The eastern solution

$$X_E = 1 - \frac{x}{r} - \frac{1}{kr}\left[1 - e^{-k(r-x)}\right], \qquad (20E)$$

$$\frac{X'_E}{k} = -\frac{1}{kr}\left[1 - e^{-k(r-x)}\right] \qquad (21E)$$

represents an exponential slippage zone of width, say, π/k (fig. 3). For $A = 5 \times 10^7$ cm^2 sec^{-1} this corresponds to roughly 200 km. This feature is likely to be obscured by meridional wind currents (section 6).

The west–east asymmetry.—The westward intensification of ocean currents[7] has been explained by Stommel (1948) as related to the planetary vorticity. The asymmetry may be expressed as either of the ratios

$$\frac{M_y(WC)}{M_y(C)} = -0.55kr; \qquad \frac{r}{x(WC)} = \frac{\sqrt{3}}{2\pi} kr$$

of the maximum western current to the central drift, or of the width of the ocean to that of the western current. The asymmetry increases with r, decreases with A and φ. For the Atlantic we found $kr \approx 100$.

But the asymmetry is not only one of narrow swift currents versus broad slow currents. The countercurrent and opposing vortices are part of the western dynamic pattern for which there is no counterpart on the eastern side of the oceans. The equivalent mathematical statement is that the real parts of the two complex roots α_1 and α_2 of the characteristic equations (16) are always negative, whereas the real roots α_3 and α_4 are positive. The leftward trend in fig. 1 of α_1' and α_2' with increasing γ shows that the asymmetry becomes even more pronounced for large zonal wind wave-numbers.

These remarks can be interpreted in terms of the differential equation of mass transport (equation 6):

$$\underbrace{\underbrace{\text{Lateral stress curl} + \text{planetary vorticity}}_{\text{western solution}} + \text{wind stress curl}}_{\text{central solution}} = 0.$$

In the central and eastern ocean areas the planetary vorticity and wind stress curl have opposite signs, and balance is achieved in which the lateral stress plays a negligible part (except in the unimportant eastern coastal zone). Along the western boundary the planetary vorticity and wind stress curl have the same sign, and the lateral stress curl balances both planetary vorticity and wind stress curl.[8] It can be verified that in this region the wind stress curl is *numerically* unimportant, although it is of course the primary cause of the circulation. The above remarks apply not only to both hemispheres, but also to the cyclonic as well as the anticyclonic gyres. The only way in which the intense currents and the boundary vortices could occur on the eastern side of the oceans would be for the earth to rotate in the opposite sense.

[7] Dynamically it is perhaps more significant to consider the concentration of virtually all the oceans' vorticity against their western shores.

[8] Stockmann (1946) has given a formal solution to (8); that is, he has neglected the important planetary vorticity.

5. Meridional wind solution

Superimposed on the eastern drift we find in various oceans rather well developed currents along the eastern boundary, the Benguela, California, Peru and Alaska currents being the outstanding examples. These currents are seasonal and vary with the winds. Since they are not contained in our solution for a zonal wind circulation we must assume that they depend on the vorticity provided by the meridional winds.

The procedure to be followed is similar to the one in section (3). The meridional wind stress in the interval $0 < x < r$ will be written as a sum of terms $\tau_{ym} = a \cos mx + b \sin mx + c$, where $m = j\pi/r$, $j = 1, 2, \cdots$ *etc.* Neglecting the effects of northern and southern boundaries, $\psi = \psi(x)$, and equation (6) reduces to

$$\left(A \frac{d^4}{dx^4} - \beta \frac{d}{dx}\right) \psi_m = -\operatorname{curl}_{zm} \tau = -\frac{d\tau_{ym}}{dx}. \qquad (6M)$$

The general solution for the m^{th} component of ψ is

$$\psi_m = \frac{\tau_{ym} - \dfrac{\delta_m^3}{m} \dfrac{d\tau_{ym}}{dx}}{k^3 A (1 + \delta_m^6)} + e^{-\frac{1}{2}kx}\left[q_1 \cos\left(\frac{\sqrt{3}}{2} kx - q_2\right) + q_3 + q_4 e^{-k(r-x)}\right], \qquad (15M)$$

where $\delta_m = m/k$ is the ratio between the meridional wind stress wave number m and the Coriolis-friction wave number $k = \sqrt[3]{\beta/A}$, and the q's are constants to be determined from the four boundary conditions (9).

In the central and eastern ocean areas ($e^{-\frac{1}{2}kx} \ll 1$) for a relatively broad meridional wind system ($\delta \ll 1$) equation (15M) gives

$$\psi(x) = \beta^{-1}[(\tau_y)_x - (\tau_y)_r + k^{-1}(\operatorname{curl}_z \tau)_r (1 - e^{-k(r-x)})], \qquad (29)$$

$$M_y(x) = \beta^{-1}[(\operatorname{curl}_z \tau)_x - (\operatorname{curl}_z \tau)_r e^{-k(r-x)}], \qquad (30)$$

independent of the wave-number m. Beyond the eastern coastal strip, (30) reduces again to Sverdrup's equation (28).

6. The California current system

Off the coast of California, perhaps as a consequence of the coastal mountain range, the usual situation is for the summer winds south of Cape Mendocino (the *Cape Horn of California*) to blow from NNW and to reach their maximum speed some distance from shore (fig. 6). Along this wind axis the curl of the wind stress changes sign, and, neglecting the very small last term in (30), the direction of transport changes sign also.

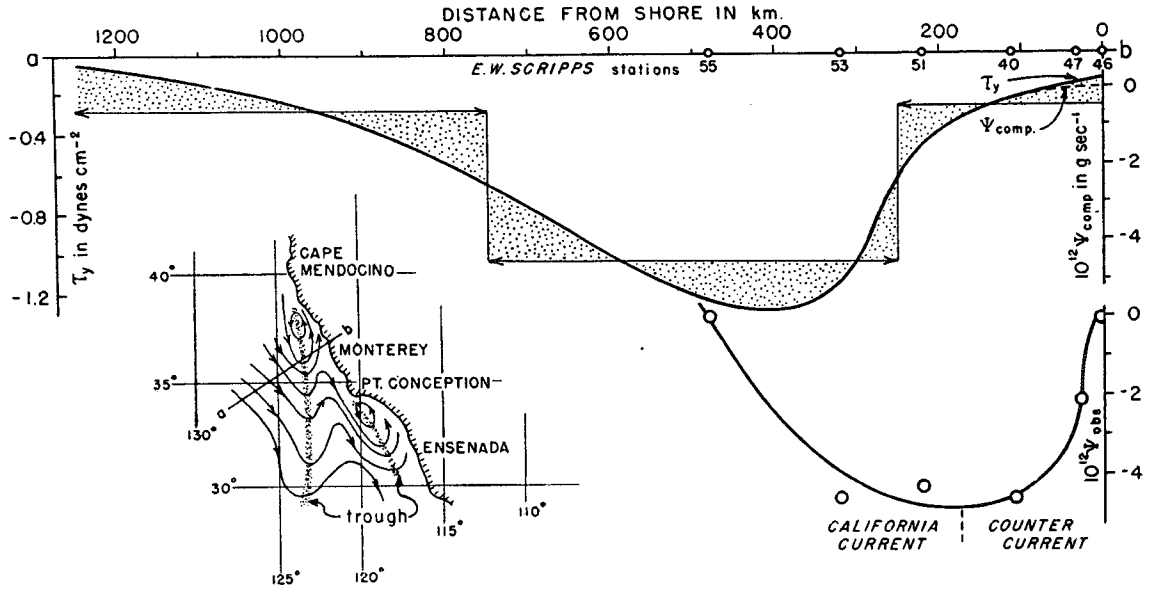

FIG. 6. Meridional winds and currents off California. Horizontal arrows in upper figure show average values of τ_y (left scale) for June over the indicated ranges along section a–b, inset. The solid curve is a rough estimate of the actual wind distribution. Except for a narrow region near shore where a slight modification is introduced by the last term in equation (30), this curve represents also the computed mass transport (right scale). The mass transport above the 1000-decibar level from oceanographic observations (Sverdrup and staff, 1942) according to equation (25) is shown by the lower curve. The inset shows dynamic height anomalies, 0 over 1000 decibar, based on observations of the *E. W. Scripps* cruise VIII, 10 May to 10 July 1939.

The existence of this biologically important countercurrent is confirmed by an oceanographic section off Monterey occupied by the *E. W. Scripps* on 11–14 June 1939 (fig. 6). The width of the current during this cruise appeared to have been considerably narrower than would be consistent with average June winds. The total transport of the countercurrent according to (29) is about 6×10^{12} g sec^{-1}; according to the oceanographic data, 5×10^{12} g sec^{-1}.

The boundary between the California Current and countercurrent represents a trough in the sea surface (inset, fig. 6) which corresponds to the axis of the northerly winds. Off the coast of Mexico, both the trough and wind axis are located further offshore. A second trough associated with an eddy south of Pt. Conception appears to be related to a second maximum of the northerly winds extending from Pt. Conception in a line with San Nicolas Island.

The foregoing application of the meridional solution suffers from the limited extent of the wind system and the lack of adequate meteorologic and oceanographic observations. All that can be said is that the average wind distribution off Monterey is consistent with the existence of a south-flowing current offshore and a countercurrent inshore, and that the computed transports of these currents compare favorably with the measured transports. It should be noted that this current-countercurrent system is a consequence of the *local* wind stress curl and dynamically altogether different from the current-countercurrent system along the western side of the oceans, which has been interpreted as a boundary phenomenon.

7. General solution

Consider now the general field of wind stress

$$\tau = \mathbf{i}\,\tau_x(x, y) + \mathbf{j}\,\tau_y(x, y)$$

associated with large-scale atmospheric circulation, *i.e.*, $\gamma \ll 1$, $\delta \ll 1$. Outside the western and eastern boundary regions, (6) then has the integral

$$\psi_C = -rX_C\beta^{-1}\,\overline{\operatorname{curl}_z \tau},$$

where X_C is given by (20C), and

$$\overline{\operatorname{curl}_z \tau} = \frac{1}{r - x}\int_x^r \operatorname{curl}_z \tau\, dx \qquad (31)$$

represents a *running* average along a segment of latitude between x and the eastern boundary. If variations of the wind stress curl with x in the western and eastern boundary regions are so gradual that ψ fluctuates essentially with $X(x)$, then

$$\psi = -rX\beta^{-1}\,\overline{\operatorname{curl}_z \tau} \qquad (32)$$

is a suitable approximation for the entire ocean area. The above condition requires $m \ll k$, which is true by hypothesis. It is in the nature of the (running) average $\overline{\operatorname{curl}_z \tau}$ that it should become the less effected by local fluctuations in the wind field the larger the value of $r - x$. This must be at least a partial explanation for the known persistency of zonal currents in the western portion of all oceans.

8. The wind-spun vortex

For a stationary, anticyclonic, circular wind system

$$\tau_\rho = 0, \qquad \tau_\theta = -\Gamma q\rho e^{-q^2\rho^2}, \qquad (33)$$

reaching a maximum stress $\Gamma/\sqrt{2e}$ at a distance from the center $\rho = \frac{1}{2}\sqrt{2}\, q^{-1}$ and zero stress at the center and at great distances, the stream function in the central ocean area (equation 20C, 31, 32) becomes

$$\psi = \beta^{-1} \int_x^\infty \text{curl}_z\, \tau\, dx$$

$$= \tfrac{1}{2}\sqrt{\pi}\, \Gamma\beta^{-1}\{[1 - 2(qy)^2][1 - I] + \tfrac{1}{2}I''\}, \quad (34)$$

where

$$I(q\rho) = \frac{2}{\sqrt{\pi}} \int_0^{q\rho} e^{-(q\rho)^2}\, d(q\rho)$$

is the probability integral and $I'' = d^2I/d(q\rho)^2$. It is assumed that the wind system essentially vanishes some distance from shore.

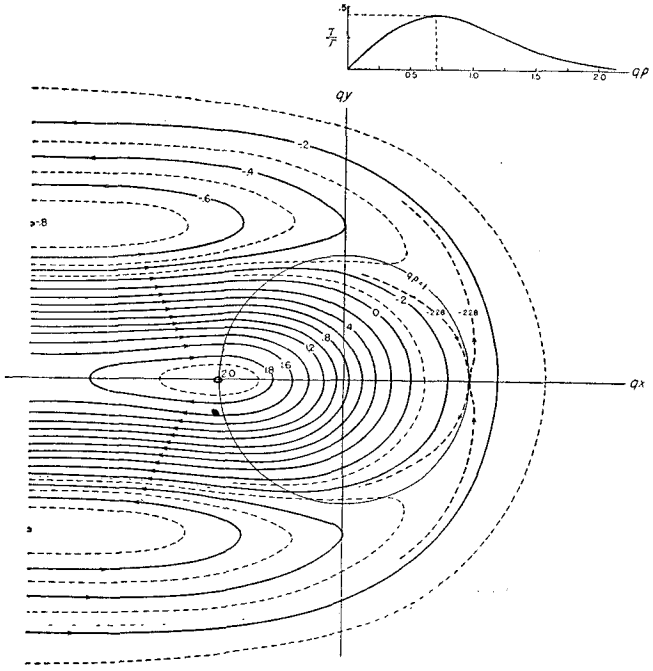

FIG. 7. Mass transport stream lines $\beta\psi/\Gamma$ (nondimensional) resulting from the circular wind system shown above.

The mass-transport streamlines (fig. 7) reveal an anticyclonic vortex centered at $-1/q$, 0, and a trough with a saddle point at $1/q$, 0. The center of the oceanic vortex is thus displaced *west* from the center of the atmospheric vortex by $\sqrt{2}$ times the radius of the maximum stress circle. The net anticyclonic circulation in the vortex is $(2.0 + .228)\Gamma/\beta = 5.2\tau_{max}/\beta$.

Meteorologic and oceanic observations in the eastern Pacific definitely show a westward displacement of the oceanic anticyclone relative to the Pacific high-pressure area with which it is associated. The magnitudes of the displacement ($\approx$1000 km) and the circulation ($\approx 20 \times 10^{12}$ g sec^{-1}) are about 60 per cent of what one might suppose on the basis of the foregoing theory. However, the lack of radial symmetry of the wind system because of its poor development in the western portion prevents a more quantitative application of the theory. The oceanographic observations are inadequate to either confirm or deny the existence of the saddle point.

It should be noticed that ψ vanishes at $x = +\infty$ but not at $x = -\infty$. This is the result of having neglected the lateral stress vorticity in dealing with the first-order equation (28) which admits only one boundary condition. For large anticyclones ($q/k \ll 1$), fig. 7 should be a good mid-ocean approximation, and one may expect a *tail* of predominately zonal currents west of the wind system, feeding water into the system north of the wind axis and expelling it south of the wind axis (vice versa for cyclones), with relatively weak compensation currents farther to the north and south. The effect of lateral stress will be to shorten the tail in proportion to the compactness of the wind system. For a wind system consisting of alternate cyclonic and anticyclonic cells over the entire globe, Goldsbrough (1935) finds a current system of similar cellular structure but displaced westward relative to the wind cells.

9. Classification of ocean currents

In writing this paper we have felt an increasing need for a general nomenclature of ocean currents, applicable in all oceans regardless of hemisphere, and suggestive of the meteorologic features to which the currents are so closely related. A possible system is proposed in fig. 8. The corresponding geographic names for all oceans are summarized in table 3. The circulation is divided into gyres, which are equivalent in scale to the climatic belts. Each gyre contains one or two *vortices* equivalent in scale to semipermanent pressure centers. It is suggested that the term *eddy* be reserved for random features associated with turbulence.

In high (north or south) latitudes the cyclonic *subpolar* gyre corresponds to the region of the cyclonic storms, the anticyclonic *subtropical* gyre to the anticyclones. The equatorial currents and countercurrent enclose two additional gyres (see fig. 2) corresponding to the trades and the doldrums, but these are so narrow that they are best not regarded as gyres. A typical gyre is composed of zonal currents to the north and south, a strong persistent current and boundary vortex on its western side, and a compensating drift in the central and eastern portion, upon which a variable eastern current and wind-spun vortex are superimposed.

The foregoing classification has chemical and biological implications (see charts IV and VI, figs. 217, 216, and 214, Sverdrup *et al.*, 1942). The subtropical gyres, for example, enclose a relatively warm, haline

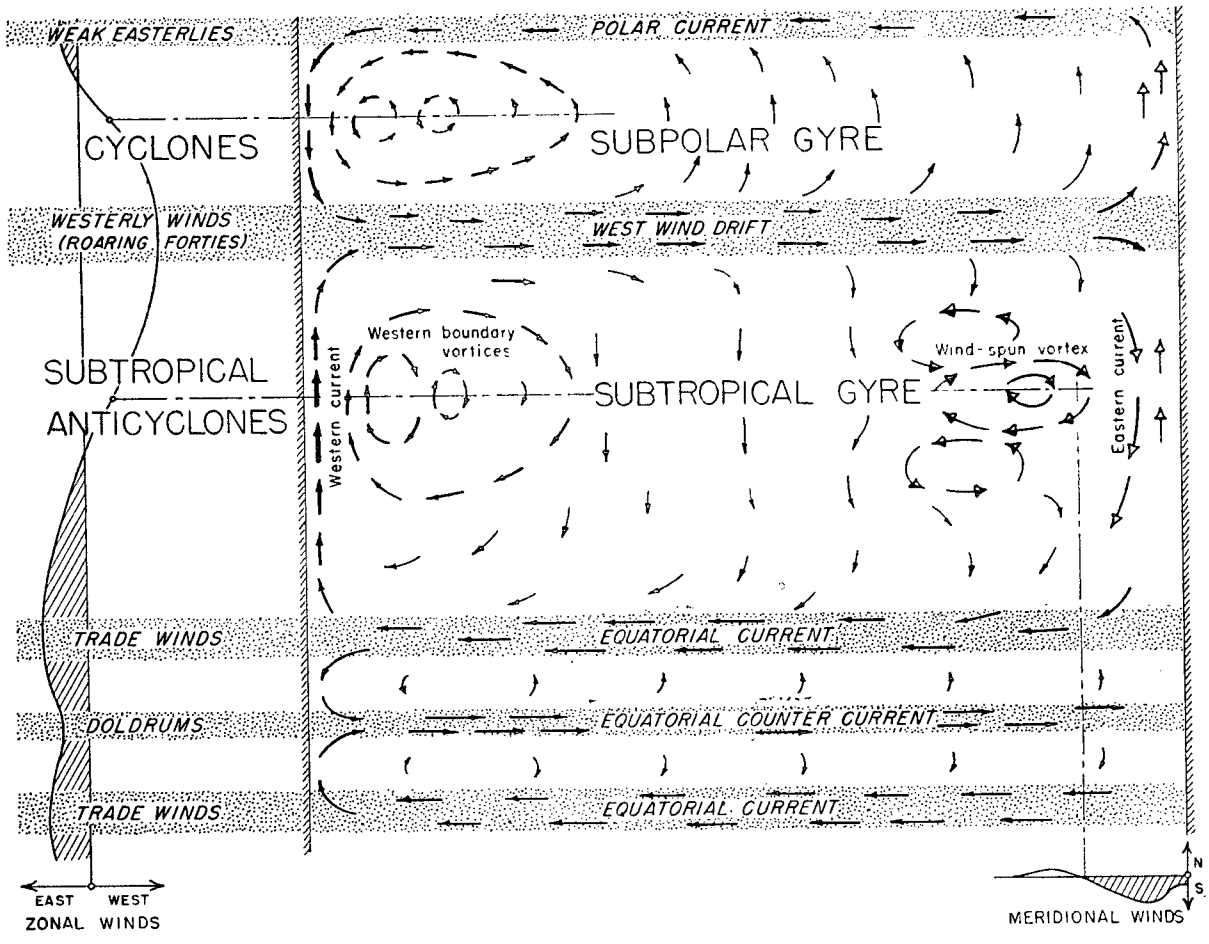

FIG. 8. Schematic presentation of circulation in a rectangular ocean resulting from zonal winds (filled arrowheads), meridional winds (open arrowheads), or both (half-filled arrowheads). The width of the arrows is an indication of the strength of the currents. The nomenclature applies to either hemisphere, but in the Southern Hemisphere the subpolar gyre is replaced largely by the Antarctic Circumpolar Current (west wind drift) flowing around the world. Geographic names of the currents in various oceans are summarized in table 3.

body of water, poor in phosphates, relatively low in biological activity, and blue in color ('blue is the desert color of the sea'). The boundaries of the gyres are marked by remarkably pronounced horizontal gradients in all these variables. The western boundary vortices are biologically unique in that they represent the only regions in the open sea where freely floating organisms in the sunlit zone can be expected to remain for any length of time in a uniform environment. Of such regions, named *halostases* by biologists, the best known is the Sargasso Sea, named after its concentration of *Sargassum*, or *Gulf Weed*, a brown alga characteristic of subtropical regions. The six remaining halostases (table 3) are equivalent dynamically to the Sargasso Sea and it would not be surprising were they also distinguished by concentrations of freely floating organisms with narrow environmental tolerance.

10. Discussion and conclusions

The classification of ocean currents in table 3 is put forth with some hesitation, as it is almost certain to include some unwarranted oversimplification. Additional data on currents and wind stress are likely to lead to revisions. Particularly in the southern oceans the boundary conditions for the subpolar gyre differ radically from those we have considered, and the dynamics of the Antarctic Circumpolar Current is not properly understood. But even so, a preliminary table is helpful in interpreting the main features in the ocean circulation and, what is more important, to point out reasons for essential *differences* in different oceans.

For example, the Gulf Stream and Brazil Current occupy equivalent positions in the North and South Atlantic, yet the Gulf Stream has about ten times as much transport. According to (26) and table 2 this difference is due chiefly to the larger wind stress curl in the North Atlantic. Differences in wind stress curl can be ascribed to the northward displacement of the climatic equator relative to the geographical equator, which reduces the distance between the trades and the westerlies in the northern hemisphere to about 60 per cent of that in the southern hemisphere. The displacement of the trades in turn seems to be related to the unequal distribution of land and sea in the two hemi-

TABLE 3. The general ocean circulation.

Classification (see fig. 8)		North Atlantic	South Atlantic	North Pacific	South Pacific	North Indian	South Indian
SUBPOLAR GYRE	POLAR CURRENT (z)		p ?	p	p (w)		p
		E. Greenland (3)					
	Western C. (z)	Labrador (6) ?	Falkland	Oyashio	a		a
	W. bdry vortex (z)	p ? (50°N, 50°W)	a ?	?	a		a
	Eastern C. (m)	Norwegian (3)	a	Alaska	a		a
	Wind-spun vortex (z, m)	a	a ?	Gulf of Alaska	a	A	a
				Aleutian (15)		S	
						I	
						A	
SUBTROPICAL GYRE	WEST WIND DRIFT (z)	GULF STREAM S.: N. Atlantic (38)	West wind drift	KUROSHIO S.: N. Pacific (20)	West wind drift		West wind drift
				Kuroshio Ext. (65)			
	Western C. (z)	Gulf Stream (70)	Brazil (7)	Kuroshio (23)	E. Australia ?		Agulhas (25)
		Florida (26)					
	W. bdry vortex (z)	Sargasso Sea	p	p	p		p
	Eastern C. (m)	Canary ?	Benguela (16)	California (15)	Peru (13)		p (v)
	Wind-spun vortex (z, m)	Azores vortex	p (30°S, 5°W)	E. Pac. vortex	p (30°S, 100°W)		p (30°S, 95°E)
	EQUATORIAL CURRENT (z)	N. Equat. C. (32)	S. Equat. C.	N. Equat. C. (45)	S. Equat. C.	N. Equat. C.	S. Equat. C.
	EQUAT. COUNTER C. (z)	Equat. C. C. (4) ←	a	Equat. C. C. (25) ←	a	a →	Equat. C. C.

a: absent; p: present, but unnamed; m: related to meridional winds; S: system; v: variable; w: weak; z: related to zonal winds.
Figures in parentheses give mass transport in 10^{12} g sec^{-1} estimated from oceanographic observations.

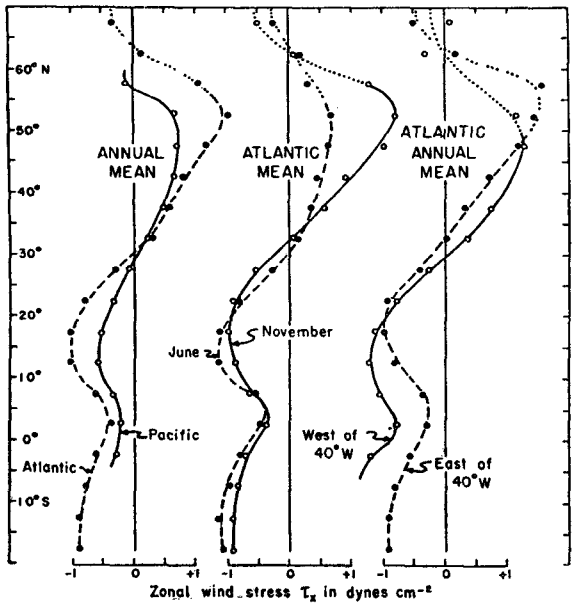

FIG. 9. Distribution of zonal wind stress with latitude. Note the longitudinal asymmetry over the North Atlantic. In the region south of Greenland, where observations are lacking, the wind stress averages have been corrected for this asymmetry. The dotted lines indicate uncertainty because of lack of sufficient observational data.

spheres. One is tempted, then, to trace the preponderance of the great Gulf Stream and Kuroshio systems over their southern counterpart to the excess of water-covered area in the southern hemisphere.

Differences in circulation between the North Atlantic and North Pacific can be at least partly ascribed to the greater intensity and northward displacement of the Atlantic zonal winds, especially during winter (fig. 9). The circulation in the subpolar gyre of the North Atlantic is complicated by two related factors: both the northern land boundaries and the axis of the westerly winds are further north in the eastern than the central and western portion. This may be the reason why the western current of the subpolar gyre is broken up into two parts (Sverdrup *et al.*, 1942, pp. 651–666): the East-Greenland current flowing at an average longitude of 30°W from 80°N to 60°N; and the Labrador current at 60°W, flowing from 60°N to 40°N.

The wind stress pattern over the subpolar gyre is largely a reflection of the traveling cyclones, and one may expect a certain adjustment of the ocean circulation to the frequency and paths of these cyclones. The extent of such an adjustment depends on the time constants of the ocean circulation. Observational evidence indicates that the adjustment to individual storms is not a major one, yet that the main currents do reveal seasonal fluctuations. The time constants appear, therefore, to be of the order of weeks, perhaps months. Thus ocean currents might represent a convenient method of obtaining time averages of atmospheric circulation. For example, the intensity of the Gulf Stream (perhaps estimated from tide records) could be related to the mean wind vorticity in the region of subtropical anticyclones over the Atlantic.

The foregoing statement is somewhat at variance with the usual assertion that the Gulf Stream is *caused* by the trades. Rather it is related to the vector *difference* between the trades and the westerlies, or, strictly speaking, to the mean value of the wind stress curl at the latitude in question. It is at least conceivable that an increase in the velocity of the trades be confined to a narrow band of latitude, and that the wind stress curl and the Gulf Stream at, say, 30°N remain unchanged. This is, however, unlikely for physical reasons as the mechanism responsible for the transfer of momentum from the westerlies to the trades would tend to distribute such an increase over the entire subtropical zone.

The validity of our statement that the intensity of the western current be proportional to the wind stress curl at the latitude in question depends on the approximations involved in neglecting the inertial terms in (1). Rossby (1936) has developed a *wake-stream theory* of the Gulf Stream in which the inertial terms play a predominant part. The theory has many attractive features. It explains the increase downstream in width and mass transport, the existence of an observed countercurrent on the *western* edge of the Gulf Stream, and a jet-like current profile which appears to be in accord with recent observations (Iselin and Fuglister, 1948).

In order to estimate the magnitude of the inertial terms it is necessary to specify the distribution of density and velocity with depth. Using Reid's exponential model for the density (23) and a similar law for the velocity:

$$v = v_0 \text{ for } -z \leqslant h', \qquad v = v_0 e^{1+z'/h} \text{ for } -z \geqslant h',$$

one obtains the expression

$$\frac{3}{8}\frac{1}{\rho_0 h'} \nabla \times (\mathbf{M}\cdot\nabla)\mathbf{M}, \tag{35}$$

to be added to the left side of the differential equation of mass transport (6). The ratio

$$\frac{\sqrt{3}}{4}\frac{r k^2 n^2 \tau_{\max}}{\rho_0 h' \beta^2} e^{-\frac{1}{2}kx} \cos\left(\frac{\sqrt{3}}{2}kx + \frac{\pi}{6}\right), \tag{36}$$

of (35) to the planetary vorticity is small except along the inshore edge of the western current, where it may reach unity. It seems likely that some of our conclusions will be modified in the sense prescribed by Rossby.

This investigation has served to emphasize the fundamental importance of the wind stress *curl* rather than of the wind stress *vector* in determining the transport of ocean currents in meridionally bounded oceans. For example, the circulation shown in figs. 2 and 6 is in no ways modified by shifting the zero axis of the

wind stress curve. It so happens that in the subtropical zone the inflection point of the zonal wind stress curve falls close to where the wind stress changes sign, and it has been tacitly assumed in most textbooks that the change from a westward to an eastward current is related to a similar change in wind direction. This general misconception probably explains the difficulty in interpreting instances where the current runs against the wind, such as the California Countercurrent, the Point Barrow Current, and most important of all, the Equatorial Countercurrent. In the case of an irrotational wind field, such as a uniform west wind, over an ocean bounded on its western and eastern sides, it follows from (4) and (22) that $\psi = 0$, $\nabla P = \tau$, *i.e.*, that there is no circulation and that the stress is balanced by the pressure distribution resulting from the piling up of water against the lee shore. With the important exception of the Antarctic Circumpolar Current, which has no major meridional boundaries, it can be stated that *permanent ocean currents are related to the rotational component of the wind stress field over the ocean. These ocean currents would vanish were the wind stress field irrotational.*

Finally we may examine the question of why the computed transports of the Gulf Stream and the Kuroshio current amount to only about one half the observed values (table 2). It does not seem reasonable that the oceanographic observations should be off by more than, say, 20 per cent, nor that the theoretical expression (26) for the transport should account for the discrepancy, since it is almost independent of the eddy viscosity and the shape of the ocean basin.

Maury and others have ascribed the North Atlantic circulation, in particular the Gulf Stream, to differential heating between equator and pole, to the freezing of ice, and to other processes that make up the *thermohaline* circulation. If we assume that the circulation were half wind-driven, half thermohaline, it would be a strange coincidence that the general *pattern* of the circulation, such as the boundaries of the gyres, should conform so closely to the general atmospheric circulation. Furthermore, Fuglister[9] has found a high correlation between *variations* in the current with variations in the wind. It should also be noted that the thermohaline circulation insofar as it is related to the outflow of river water along the Atlantic seaboard would tend to reduce rather than to strengthen the Gulf Stream. It would seem therefore that the subtropical gyre, and probably also the subpolar gyre, are predominantly wind-driven.

Methods for computing wind stress from the observed wind speeds according to the equation

$$\tau = C_D \rho_{air} U^2$$

are discussed by Reid (1948a) and in SIO Oceanographic Report 14.[10] Underestimates of τ may first of all result from underestimates in the wind speeds on the climatological charts from which the appropriate averages were taken. The preponderance of coastal stations, and the tendency of ships at sea to avoid regions of high wind, would lead to consistent errors, but these cannot account for more than a fraction of the discrepancies. The weakest link is the drag coefficient C_D which is based on measurements of Baltic storm tides, and a few other measurements (Sverdrup *et al.*, 1942, pp. 489–500). In accordance with the views presently accepted we have assumed $C_D = .0026$ at high wind speeds, $C_D \approx .008$ at low speeds, with the discontinuity occurring at Beaufort 4 (Munk, 1947). In the trade-wind belt of the eastern Pacific, where the winds are predominantly Beaufort 4 and above, Sverdrup (1947) and Reid (1948a) have obtained satisfactory agreement between computed and observed transports. Supposing a value of .0026 were applicable at all wind speeds, then the effect of the southwesterly winds over the eastern Atlantic would make itself felt in a much higher meridional wind factor (table 2), and it can be demonstrated that the discrepancy between computed and observed transports could be largely accounted for. We are therefore led to propose a higher value of C_D at low wind speeds.[11] The transports of the Gulf Stream and Kuroshio current are, after all, probably as good an indicator of the overall stress exerted by the winds on the ocean as any of the measurements on which the value of C_D is now based.

Acknowledgments.—The writer has benefited greatly by many discussion with Einar Høiland of the Institute of Theoretical Astrophysics, University of Oslo, where most of this paper was prepared. Drs. H. U. Sverdrup, C.-G. Rossby and C. E. Eckart have made many helpful suggestions. The tedious computations of wind stress have been performed by Jo Nixon and Viola Bush under the supervision of Robert Reid, John Cochrane and Palmer Osborn, as part of a research project sponsored by the Office of Naval Research. The writer is also deeply indebted to the Guggenheim Foundation for its generous support.

REFERENCES

Defant, A., 1941: Die absolute Topographie des physikalischen Meeresniveaus und der Druckflächen, sowie die Wasserbewegungen im Atlantischen Ozean. *Deutsche Atlantische Expedition METEOR 1925–1927, Wiss. Erg.*, 6, No. 2/5, fig. 41.

[9] F. C. Fuglister, "Annual variations in current speeds in the Gulf Stream system," *Woods Hole Oceanographic Institution Technical Report No. 15* (unpublished), 1948.

[10] Scripps Institution of Oceanography, "The field of mean wind stress over the North Pacific Ocean," Oceanographic Report No. 14 (unpublished).

[11] Neumann (1948) claims on the basis of his analysis of Baltic and North Sea tilt that the drag coefficient actually *increases* with decreasing wind speed. His average value for C_D pertaining to Beaufort 3 is in excess of .0040.

Ekman, V. W., 1923: Über Horizontalzirkulation bei winderzeugten Meeresströmungen. *Arkiv Mat. Astr. Fysik*, **17**, No. 26, 74 pp.

Ekman, V. W., 1932: Studien zur Dynamik der Meeresströmungen. *Gerlands Beitr. Geophysik*, **36**, 385–438.

Felber, O-H., 1934: Oberflächenströmungen des Nordatlantischen Ozeans zwischen 15° and 50°N.B. *Arch. Deutschen Seewarte*, **53**, 2–50.

Goldsbrough, G. R., 1935: On ocean currents produced by winds. *Proc. roy. Soc. London.* (A), **148**, 47–58.

Hidaka, K., 1949: Mass transport in ocean currents and lateral mixing. *J. marine Res.*, **8**, 1932–36.

Iselin, C. O'D., 1936: A study of the circulation of the western North Atlantic. *Pap. phys. Ocean. Meteor., Mass. Inst. Tech. and Woods Hole ocean Instn.*, **4**, No. 4, 101 pp.

Iselin, C. O'D., and F. C. Fuglister, 1948: Some recent developments in the study of the Gulf Stream. *J. Marine Res.*, **7**, 317–329. (Sverdrup Anniv. Vol.)

Love, A. E. H., 1944: *A treatise on the mathematical theory of elasticity.* Fourth Ed., Dover, New York, 643 pp.

Montgomery, R. B., 1939: Ein Versuch, den vertikalen und seitlichen Austausch in der Tiefe der Sprungschichte im äquatorialen Atlantischen Ozean zu bestimmen. *Ann. Hydrogr. mar. Meteor.*, **67**, 242–246.

Munk, W. H., and G. F. Carrier, 1950: The wind-driven circulation in ocean basins of various shapes. *Tellus* (in press).

Munk, W. H., 1947: A critical wind speed for air-sea boundary processes. *J. Marine Res.*, **6**, 203–218.

Neumann, G., 1948: Über den Tangentialdruck des Windes und die Rauhigkeit der Meeresoberfläche. *Z. f. Meteor.*, **2**, 193–203.

Rayleigh, Lord, 1893: On the flow of viscous fluids, especially in two dimensions. *Phil. Mag.* (5), **36**, 354–372.

Reid, R. O., 1948a: The equatorial currents of the eastern Pacific as maintained by the stress of the wind. *J. Marine Res.*, **7**, 74–99.

Reid, R. O., 1948b: A model of the vertical structure of mass in equatorial wind-driven currents of a baroclinic ocean. *J. Marine Res.*, **7**, 304–312. (Sverdrup Anniv. Vol.)

Rossby, C.-C., 1936: Dynamics of steady ocean currents in the light of experimental fluid mechanics. *Pap. phys. Ocean. Meteor., Mass. Inst. Tech. & Woods Hole ocean. Instn.*, **5**, No. 1, 43 pp.

Stockmann, W. B., 1946: Equations for a field of total flow induced by the wind in a non-homogeneous sea. *C. R. Acad. Sci. URSS.*, **54**, 403–406.

Stommel, H., 1948: The westward intensification of wind-driven ocean currents. *Trans. Amer. geophys. Union*, **29**, 202–206.

Sverdrup, H. U., and staff, 1942: Oceanographic observations on the "E. W. SCRIPPS" cruises of 1938. *Records of observations*, Scripps Inst. Ocean., **1**, 1–64.

Sverdrup, H. U., M. W. Johnson, and R. H. Fleming, 1942: *The Oceans, their physics, chemistry, and general biology.* Prentice-Hall, New York, 1087 pp.

Sverdrup, H. U., 1947: Wind-driven currents in a baroclinic ocean; with application to the equatorial currents of the eastern Pacific. *Proc. Nat. Acad. Sci.*, **33**, 318–326.

Uda, M., 1938: Hydrographical fluctuation in the northeastern sea-region adjacent to Japan of North Pacific Ocean. *Japan, Imper. Fisheries Sta., Jour.*, **9**, 64–85.

Wüst, G., 1936: Kuroshio and Golfstrom. *Berlin Univ., Inst. f. Meereskunde, Veröff., N. F.*, A. Geogr.-Naturwiss., **29**, 69 pp.